SCIENTIFIC REPORTS

OPEN

SUBJECT AREAS:
TARGETED THERAPIES
BREAST CANCER

Received
12 October 2014

Accepted
16 December 2014

Published
26 January 2015

Correspondence and requests for materials should be addressed to J.Z. (zhjq@seu.edu.cn)

Enhanced antitumor effects of the BRBP1 compound peptide BRBP1-TAT-KLA on human brain metastatic breast cancer

Bo Fu[1], Wei Long[1], Ying Zhang[1], Aifeng Zhang[1], Fengqin Miao[1], Yuqing Shen[1], Ning Pan[1], Guangming Gan[1], Fang Nie[2], Youji He[1], Jianqiong Zhang[1] & Gaojun Teng[2]

[1]Key Laboratory of Developmental Genes and Human Disease, Ministry of Education; Medical School, Southeast University, Nanjing, China, [2]Jiangsu Key Laboratory of Molecular and Functional Imaging; Department of Radiology, Zhongda Hospital; Medical School, Southeast University, Nanjing, China.

Novel molecularly targeted agents that block the development and metastasis of human brain metastatic breast cancer hold great promise for their translational value. In this study, we constructed a novel targeting composite peptide BRBP1-TAT-KLA comprising of three elements: a brain metastatic breast carcinoma cell (231-BR)-binding peptide BRBP1, a cell penetrating peptide TAT, and a proapoptotic peptide KLA. This composite peptide efficiently internalized in 231-BR cells and consequently induced mitochondrial damage and cellular apoptosis. Exposure of 231-BR cells to BRBP1-TAT-KLA significantly decreased cell viability and increased apoptosis compared with the cells treated with the control peptides. *In vivo* relevance of these findings was further corroborated in the 231-BR tumor-bearing mice that demonstrated significantly delayed tumor development and metastasis following administration of BRBP1-TAT-KLA compared with those treated with TAT-KLA alone. Interestingly, BRBP1-TAT-KLA inhibited the formation of both large and micro-metastases, while TAT-KLA alone failed to significantly reduce micro-metastases in the breast cancer brain metastasis mice. BRBP1-TAT-KLA selectively homed to the tumors *in vivo* where it induced cellular apoptosis without significant toxicity on non-tumor tissues. Our findings therefore demonstrated the enhanced antitumor effects of the BRBP1 compound peptide BRBP1-TAT-KLA, providing insights toward development of a potential therapeutic strategy for brain metastatic breast cancer.

Metastatic brain tumors represent the most common cerebral neoplasm in adults and breast cancer is the second most common solid malignancy that metastasizes to the brain[1,2]. Brain metastases are a leading cause of morbidity and mortality, affecting survival, neurocognition, speech, coordination, behavior, and quality of life[3]. Currently, whole brain radiation therapy (WBRT), surgery, and stereotactic radiosurgery (SRS) remain the standard of care for patients with brain metastases[4]. However, severe side-effects of radiotherapies and the fact that surgical resection is only used for patients with limited extracranial metastases or a single brain lesion, renders the clinical therapies of breast cancer brain metastases problematic[5–7]. Development of novel agents that specifically target the brain metastatic breast cancer is therefore urgently warranted in the field for improved treatment of breast cancer related brain metastatic tumor.

It is well-recognized that there are specific homing molecules that mediate organ-specific metastasis formation on the heterogeneous tumor cell surface[8]. Special features of tumor cells enables a molecularly targeted therapeutic strategy. Tumor-targeting ligands such as peptides and antibodies may effectively aid certain cytotoxic agents (either biological or synthetic) to deliver to the tumor cells, thereby improving therapeutic efficacy while limiting the exposure of normal tissues to the cytotoxic agents[9]. Short peptides, as targeted drug delivery vehicles, appear to have some advantages owing to their small size, efficient tissue penetrability, and minimal toxicity and immunogenicity[10]. In our previous study, we identified a linear dodecapeptide peptide, BRBP1 (MYPWTEPSYLSN), through random peptide phage display bio-panning against the human "brain-seeking" breast carcinoma cells (231-BR cells)[11]. The peptide preferentially bound to 231-BR cells in a concentration-dependent and energy-dependent manner *in vitro*. Using the near-infrared fluorophores (NIRF) imaging, we also demonstrated that there was accumulation of BRBP1 in the tumors *in vivo* following tail vein injection. Since BRBP1 was able to bind specifically to the brain metastatic breast cancer both *in vitro* and *in vivo*, we hypothesized that this peptide could potentially be applicable for delivery of cytotoxic agent(s) to the intended tumor.

Mounting evidence suggest that the mitochondrion is one of the important therapeutic targets for tumors[12–16]. Dysfunction of mitochondria is known to trigger cell death signaling cascades and mitochondria-dependent apoptosis[17,18]. KLA, a typical amphiphilic α-helical proapoptotic peptide, with the amino acid sequence of $D(KLAKLAK)_2$, can initiate apoptosis in mammalian cells via disruption of the mitochondrial membrane[19,20]. However, KLA is not plasma membrane-permeable and thus requires facilitated intracellular delivery for optimal activity[21]. The transactivator of transcription (TAT) peptide, 47YGRKKRRQRRR57, derived from the human immunodeficiency virus type 1 (HIV-1) Tat protein, is a most commonly used cell penetrating peptide (CPPs)[22]. Since TAT is a positively charged arginine-rich peptide, it can translocate cargoes not only across the cell membrane but also into the mitochondrial matrix[23]. Therefore, by conjugating KLA with TAT, the resulting TAT-KLA peptide that can cross the plasma membrane and in doing so, preferentially disrupts the negatively charged mitochondrial membranes, can exhibit cytotoxicity both *in vitro* and *in vivo*[24].

Although TAT-KLA has been used previously in the study of cancers such as melanoma tumor and lung carcinoma therapies[24,25], a major drawback of this peptide is its non-specificity for tumor cells, often leading to negative adverse effects[26]. We thus hypothesized that the inclusion of BRBP1 peptide could enhance the binding of TAT-KLA to the brain metastatic breast cancer cells, allowing for targeted antitumor therapy. In this study, we examined the enhanced antitumor activity of BRBP1-TAT-KLA on brain metastatic breast cancer both *in vitro* and *in vivo*, thereby providing evidence for the efficacy of this novel strategy for a targeted therapy against breast cancer related metastatic brain tumor.

Results

Effect of BRBP1-TAT-KLA on tumor cell activity *in vitro*. Human "brain-seeking" breast carcinoma cells (231-BR), with 100% brain metastasis efficiency[27,28], were isolated from the MDA-MB-231 human breast carcinoma cells by successive rounds of *in vivo* selection and *ex vivo* culturing[29]. Our previous study identified a phage display-derived peptide BRBP1 (MYPWTEPSYLSN) that demonstrated preferentially binding to 231-BR cells[11]. In order to develop a targeted agent for improved brain metastatic breast cancer therapy, we set up a targeting composite peptide system (BRBP1-TAT-KLA) that comprised of KLA peptide as the drug, TAT as a plasma membrane translocation unit, and BRBP1 as a targeting element. The structural model of this composite peptide is demonstrated in Figure 1a.

Firstly, we sought to examine the effect of BRBP1-TAT-KLA on cell viability *in vitro* using the MTT assay. As shown in Figure 1b, BRBP1-TAT-KLA at the concentrations of both 10 μM and 20 μM significantly decreased the viability of 231-BR cells ($P < 0.05$). Although TAT-KLA alone also exerted cytoxicity against 231-BR cells, there was higher inhibition induced by BRBP1-TAT-KLA compared with TAT-KLA alone (69.55 ± 5.70% *vs* 49.76 ± 4.60%, $P = 0.012$). BRBP1, KLA, or BRBP1-KLA alone failed to exert significant effect on the viability of 231-BR cells (Figure 1b). Additionally, treatment of MDA-MB-231 and BT-474 breast cancer cells with BRBP1-TAT-KLA at the concentration of 20 μM resulted in a greater inhibition of cell viability compared with the cells exposed to TAT-KLA alone ($P = 0.024$ and 0.028, respectively; Supplementary Figure S1a and S1b). Furthermore, BRBP1-TAT-KLA at the concentration of 20 μM failed to elicit greater inhibition of proliferation of the human breast cancer cells MCF7 ($P = 0.086$; Supplementary Figure S1c), normal mammary epithelial cells MCF 10A ($P = 0.926$; Supplementary Figure S1d), or human normal hepatic immortal cells HL-7702 ($P = 0.964$; Figure 1c) comapred with the cells treated with the TAT-KLA peptide alone.

Having determined the decreased cell viability induced by BRBP1-TAT-KLA, we next wanted to examine the effect of BRBP1-TAT-KLA on cellular death. As shown in Figure 1d and 1e, treatment of 231-BR cells with BRBP1-TAT-KLA (20 μM) induced cell swelling. TUNEL staining demonstrated that exposure of the cells to BRBP1-TAT-KLA (20 μM) resulted in a higher percentage of cellular apoptosis compared with the cells treated with dimethyl sulfoxide (DMSO; vehicle control), BRBP1, KLA, BRBP1-KLA, or TAT-KLA ($P < 0.001$; Supplementary Figure S2). This finding was further validated by FACS assay using the Annexin V-FITC/Propidium Iodide (PI) staining (Figure 1f and 1g). While both BRBP1-TAT-KLA and TAT-KLA induced cellular apoptosis, there was a higher percentage of apoptosis induced by BRBP1-TAT-KLA compared with TAT-KLA (25.85 ± 2.84% *vs* 17.80 ± 1.50%, $P = 0.005$; Figure 1f and 1g). Cumulatively, these findings suggested that BRBP1-TAT-KLA decreased 231-BR cell viability and also increased cellular death *in vitro*.

Internalization of BRBP1-TAT-KLA in 231-BR cells triggered mitochondria-mediated cellular apoptosis. Internalization of KLA has been shown to play a critical role in cytotoxicity[19,30,31]. To explore the mechanism(s) underlying the cytotoxicity induced by BRBP1-TAT-KLA, we first sought to investigate whether this peptide could internalize in 231-BR cells, using the Z-stack fluorescence confocal microscopy. As shown in Figure 2a, following 30 min of incubation with 231-BR cells, BRBP1-TAT-KLA primarily located in the cytoplasm, but not around the cell membrane or in the nucleus, indicating efficient internalization of this composite peptide in living cells *in vitro*.

Following internalization, the next logical step was to examine the effect of BRBP1-TAT-KLA on mitochondrial morphology and cellular apoptosis. 231-BR cells were exposed to varying concentrations of BRBP1-TAT-KLA, and cellular ultrastructural changes were observed by transmission electron microscopy (TEM). As shown in Figure 2b, compared with the control group, exposure of 231-BR cells to BRBP1-TAT-KLA (10 μM) for 6 h induced typical enlarged matrix compartments and prominent cristae. When the cells were treated with a higher concentration of BRBP1-TAT-KLA (20 μM), mitochondrial damage progressed appearing as swollen vesicle-like structures. In addition to mitochondrial abnormalities, autophagosomes (red arrows) which contain membranous whorls or electron-dense organelles, were also evident. When the concentration of BRBP1-TAT-KLA was raised to 30 μM, extremely swollen vesicle-like structures of mitochondria were evident and the cells progressed to the final stages of apoptosis as characterized by the presence of extensive vacuolization and karyopyknosis. These data thus demonstrated that BRBP1-TAT-KLA induced abnormal mitochondrial changes and cellular apoptosis in a concentration-dependent manner following its internalization in 231-BR cells.

Previous work has suggested that internalization of KLA peptide leads to cellular apoptosis by disrupting mitochondrial homeostasis and activating caspases[19]. Caspase-activating proteins (cytochrome c) released from damaged mitochondria in turn, induce activation of caspases 9 and 3[20,31]. Having determined that BRBP1-TAT-KLA induced mitochondrial damage and cellular apoptosis, we next sought to confirm the activation of mitochondria-mediated apoptotic pathway. 231-BR cells were treated with varying concentrations of BRBP1-TAT-KLA (10 μM and 20 μM) for 12 h followed by assessment of caspases 9 and 3 activation by western blotting. As shown in Figure 2c and 2d, treatment of 231-BR cells with BRBP1-TAT-KLA resulted in significant cleavage of caspases 9 and 3 compared with the control group, suggesting thereby that caspases activation could in part, be involved in BRBP1-TAT-KLA mediated effects on cell viability.

BRBP1-TAT-KLA inhibited tumor cell migration *in vitro*. Based on a previous study by Ma *et al.*[30] that KLA coupled peptides could inhibit the invasiveness of tumor cells *in vitro*, we next sought to examine the effect of BRBP1-TAT-KLA on cell migration. 231-BR

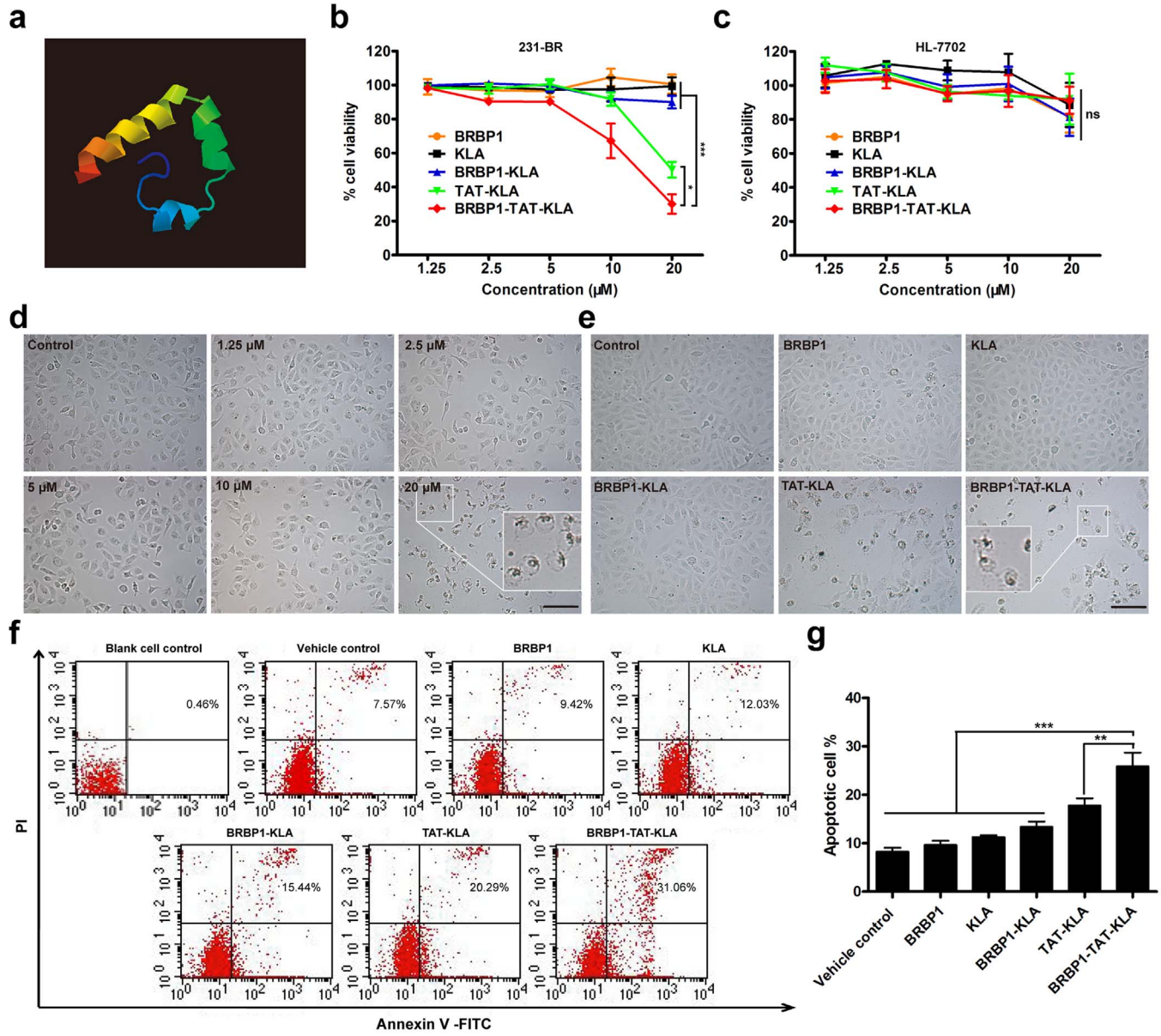

Figure 1 | ***In vitro*** **cytotoxicity of the BRBP1-TAT-KLA peptide.** (a) The structural model of BRBP1-TAT-KLA predicted and generated by the I-TASSER server. (b) and (c) Effect of BRBP1-TAT-KLA on cell viability. 231-BR (b) and HL-7702 (c) cells were treated with BRBP1, KLA, BRBP1-KLA, TAT-KLA, or BRBP1-TAT-KLA for 48 h at varying concentrations, followed by measurement of the cytotoxicity using the MTT assay. Data are represented as mean ± SEM. 231-BR, n = 4; HL-7702, n = 3. *, $P < 0.05$; ***, $P < 0.001$; ns, not significant. (d) and (e) Effect of BRBP1-TAT-KLA on cellular morphology. 231-BR cells were treated with BRBP1-TAT-KLA at varying concentrations (d) or BRBP1, KLA, BRBP1-KLA, TAT-KLA, and BRBP1-TAT-KLA at the concentration of 20 μM (e) for 24 h, respectively. Scale bars represent 50 μm. (f) and (g) Effect of BRBP1-TAT-KLA on cellular apoptosis. 231-BR cells were incubated with DMSO (vehicle control), BRBP1, KLA, BRBP1-KLA, TAT-KLA, or BRBP1-TAT-KLA for 6 h and then the apoptosis rate was assessed by Annexin V-FITC/PI staining. (g) The quantification of cell apoptosis rates (early and late apoptosis) are represented as mean ± SEM for three separate experiments. **, $P < 0.01$; ***, $P < 0.001$.

cells were treated with BRBP1-TAT-KLA at concentrations of 1.25 μM and 2.5 μM and assessed for cell migration using a transwell system. As shown in Figure 3a and 3b, BRBP1-TAT-KLA at concentrations of 1.25 μM and 2.5 μM significantly inhibited the cell migration up to 43.23% ($P = 0.015$) and 60.89% ($P = 0.002$), respectively, compared with the control group. The rationale for choosing these two concentrations of BRBP1-TAT-KLA was based on the fact that at these concentrations the peptide was determined to be below the threshold for reducing cell viability (98.33 ± 0.17% and 90.43 ± 0.29%, respectively; Figure 1b). These findings thus indicated that BRBP1-TAT-KLA inhibited migration of 231-BR cells *in vitro*.

BRBP1-TAT-KLA homed to the tumor *in vivo*. A prerequisite for the use of a targeting agent is its selective homing to the targeted cancerous tissues and limited uptake by normal tissues[32,33]. For *in vivo* validation of the tumor targeting activity of BRBP1-TAT-KLA, 231-BR subcutaneous tumor-bearing mice were generated and intravenously (i.v) injected with the peptide (1 nmol) through the tail vein. As shown in Figure 4a, compared with TAT-KLA, distribution of BRBP1-TAT-KLA was primarily restricted to the 231-BR tumors with only a limited amount of them was distributed in the normal organs, such as the heart, lung, and kidney.

Next, we sought to investigate the brain metastases targeting ability of BRBP1-TAT-KLA. The breast cancer brain metastasis mice

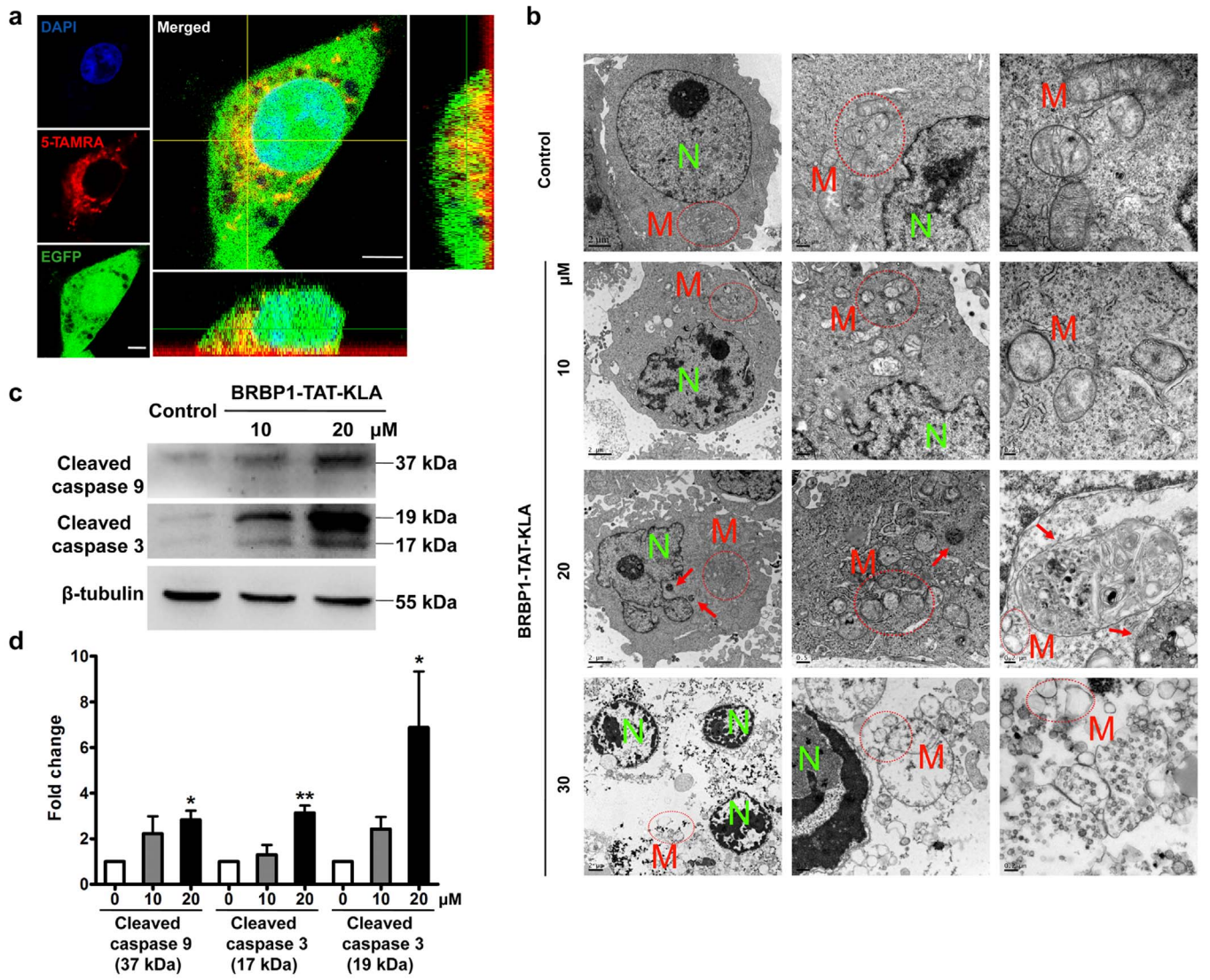

Figure 2 | BRBP1-TAT-KLA internalized in 231-BR cells and induced mitochondrial damage and cellular apoptosis. (a) Cellular uptake and internalization of BRBP1-TAT-KLA. Z-stack confocal imaging of 231-BR(EGFP) cells (EGFP, green) treated with BRBP1-TAT-KLA (5-TAMRA, red) shows the internalization of the peptide. The cell nucleus were counterstained with DAPI (blue). The images represent a single image slice taken from the z-series toward the center of the cell. The middle bottom image is a projection through the entire z-series at the horizontal line and the right image is a projection through the entire z-series at the vertical line. Scale bars represent 5 μm. (b) BRBP1-TAT-KLA induced cellular ultrastructural changes. 231-BR cells treated with BRBP1-TAT-KLA at varying concentrations (10 μM, 20 μM, and 30 μM). The ultrastructural changes were observed using TEM, compared with the untreated tumor cells (Control). M, mitochondria; N, nucleus; Red circles, highlighted mitochondria; Red arrows, autophagosomes. (c) and (d) BRBP1-TAT-KLA induced cellular apoptosis involving caspases 9 and 3 activation. 231-BR cells were treated with 10 μM or 20 μM BRBP1-TAT-KLA for 12 h, followed by collection of the total proteins to detect the cleavage of caspases 9 and 3 by western blotting. Representative immunoblots (c) and the densitometric analysis (d) of cleaved caspases 9 and 3 from three separate experiments are presented. Data are indicated as mean ± SEM. *, $P < 0.05$; **, $P < 0.01$ versus the control group.

were generated and i.v injected with 1 nmol of BRBP1-TAT-KLA. As shown in Figure 4b, compared with TAT-KLA, there was increased distrubution of the fluorescence intensity in the brain metastasis lesions in the BRBP1-TAT-KLA peptide-treated group. Moreover, BRBP1-TAT-KLA mainly homed to the brain metastases areas while negligible amounts homed to the normal brain tissues. Together, these findings underscore the tumor-targeting ability of BRBP1-TAT-KLA *in vivo*.

BRBP1-TAT-KLA inhibited tumor growth and outgrowth to the brain *in vivo*. Having determined the tumor-targeting ability of BRBP1-TAT-KLA *in vivo*, we next wanted to examine whether this peptide could inhibit tumor growth in mice. The 231-BR subcutaneous tumor mice were i.v injected with 50 nmol of either BRBP1-TAT-KLA or TAT-KLA every three days for the period of three weeks. Tumor growth was significantly inhibited in the BRBP1-TAT-KLA peptide-treated mice compared with the mice treated with either TAT-KLA or the control group ($P = 0.020$ and $P < 0.001$, respectively; Figure 5a and 5b). As reproted in previous study[24], TAT-KLA has shown a trend toward slowing tumor growth in the tumor-bearing mice, however, there was increased tumor growth inhibition in the BRBP1-TAT-KLA peptide-treated group compared with the TAT-KLA peptide-treated group ($P = 0.020$; Figure 5b).

We next sought to explore whether there was the possibility that BRBP1-TAT-KLA could function as a preventive or therapeutic agent to suppress the outgrowth of 231-BR cells to the brains in mice. Breast cancer brain metastasis mice were i.v injected with 50 nmol of

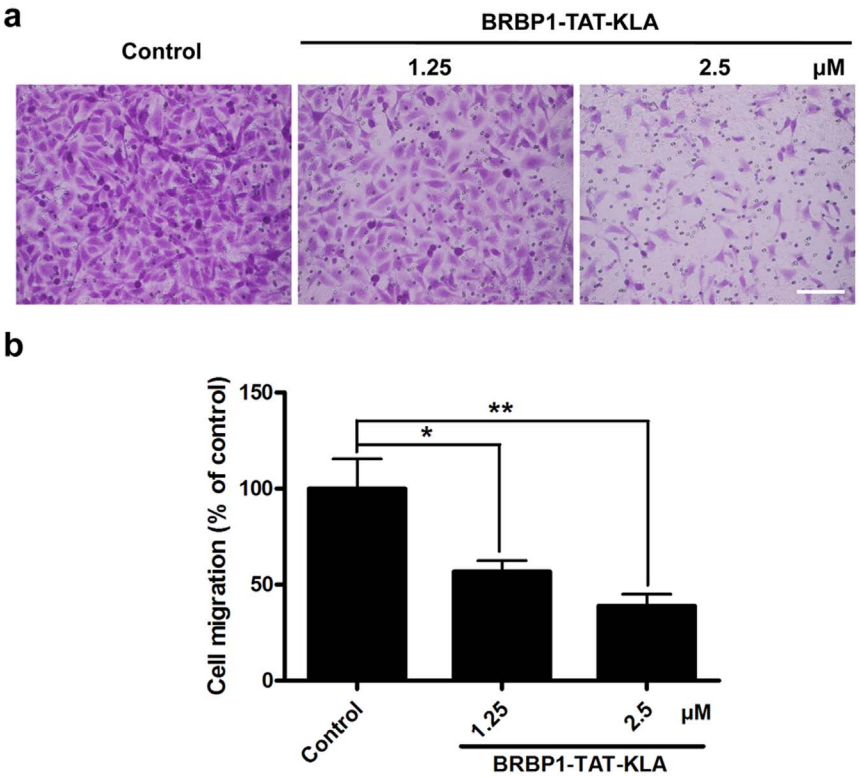

Figure 3 | BRBP1-TAT-KLA inhibited the migration of 231-BR cells *in vitro*. The cells were treated with 1.25 μM or 2.5 μM BRBP1-TAT-KLA for 30 min and subsequently the cell migration was assessed in a transwell system. (a) Representative images of migrated 231-BR cells. Scale bar represents 50 μm. (b) Quantification of the percentage of the migrated cells. Data are represented as mean ± SEM for four separate experiments. *, $P < 0.05$; **, $P < 0.01$.

peptides (BRBP1-TAT-KLA or TAT-KLA) every other day. Four weeks later, brain metastatic lesions were detected in the live mice using magnetic resonance (MR) imaging. As shown in Figure 5c, BRBP1-TAT-KLA treatment significantly suppressed the tumor outgrowth compared with the mice treated with TAT-KLA alone or the control group. This finding was further confirmed using *ex vivo* fluorescence imaging as evidenced by the fact that there was lower fluorescence intensity in the BRBP1-TAT-KLA peptide-treated mice compared with either the TAT-KLA peptide-treated or the control group (Figure 5d). In order to further assess the effect of BRBP1-TAT-KLA on the outgrowth of 231-BR cells to the brain, numbers of large metastases (>50 μm^2) and micro-metastases (≤ 50 μm^2) (Figure 5e) were quantified in the hematoxylin and eosin (H&E)-stained serial brain sections as described previously[27,34,35]. As shown in Figure 5f–h, TAT-KLA treatment only significantly reduced the large metastases ($P = 0.049$; Figure 5g) while showing no significant effect on the number of micro-metastases ($P = 0.209$; Figure 5h) compared with the control group. Mice treatment with BRBP1-TAT-KLA showed a remarkable decrease in the number of both large metastases and micro-metastases compared with the TAT-KLA peptide-treated group ($P = 0.031$ and 0.048, respectively; Figure 5g and 5h) and the control group ($P = 0.006$ and 0.010, respectively; Figure 5g and 5h). Collectively, these findings demonstrated that BRBP1-TAT-KLA significantly inhibited tumor growth and outgrowth to the brain *in vivo*.

Evaluation of apoptosis and potential side-effects in the BRBP1-TAT-KLA peptide-treated mice. Having determined that BRBP1-TAT-KLA selectively targeted the tumor tissues and efficiently inhibited tumor growth, we next sought to investigate whether this peptide could induce apoptosis in the xenograft 231-BR tumors *in vivo* using TUNEL assay. As shown in Figure 6a and 6b, the percentage of apoptotic cells in the tumor tissue was significantly increased in the BRBP1-TAT-KLA peptide-treated mice compared with the mice treated with TAT-KLA (9.60 ± 2.39% *vs* 5.53 ± 1.84%, $P = 0.012$), indicating thereby that BRBP1-TAT-KLA significantly induced cellular apoptosis in the tumor tissue *in vivo*.

One of the major disadvantages of current anticancer therapies is the side-effects on normal tissues[32]. To examine whether BRBP1-TAT-KLA induced adverse effects, histological changes in the normal tissues were assessed by H&E staining at the end of treatment. In the BRBP1-TAT-KLA peptide-treated mice there were no apparent histological changes in the tissue sections of heart, liver, spleen, lung, and kidney compared with the control group (Figure 6c and Supplementary Figure S3). Collectively, these data thus demonstrated that BRBP1-TAT-KLA induced cellular apoptosis in the tumor without significant cell toxicity against normal tissues *in vivo*.

Discussion

Brain metastasis is a devastating neurological complication accompanying systemic cancers. There is an urgent need for the development of therapeutic agents with high specificity and low side-effects for brain metastatic breast cancer[27,34]. In this study, we developed a molecularly targeted composite peptide BRBP1-TAT-KLA for improved treatment of brain metastatic breast cancer. This peptide is composed of three modular (targeting, transduction and proapoptosis) domains: (i) BRBP1, a brain metastatic breast cancer cell binding peptide, improves the specificity of therapeutic agents for cancer cells and thereby achieves optimized therapeutic efficiency; (ii) TAT, a cell penetrating peptide, acts as a vehicle that traverses the plasma membrane and mitochondrial membrane barriers and thus delivering therapeutic agents within the cells; (iii) KLA, a proapoptotic peptide, induces mitochondrial damage and triggers mitochondria-mediated apoptosis following its uptaken by the cells. These three domains confer each of their properties co-operatively to the fused

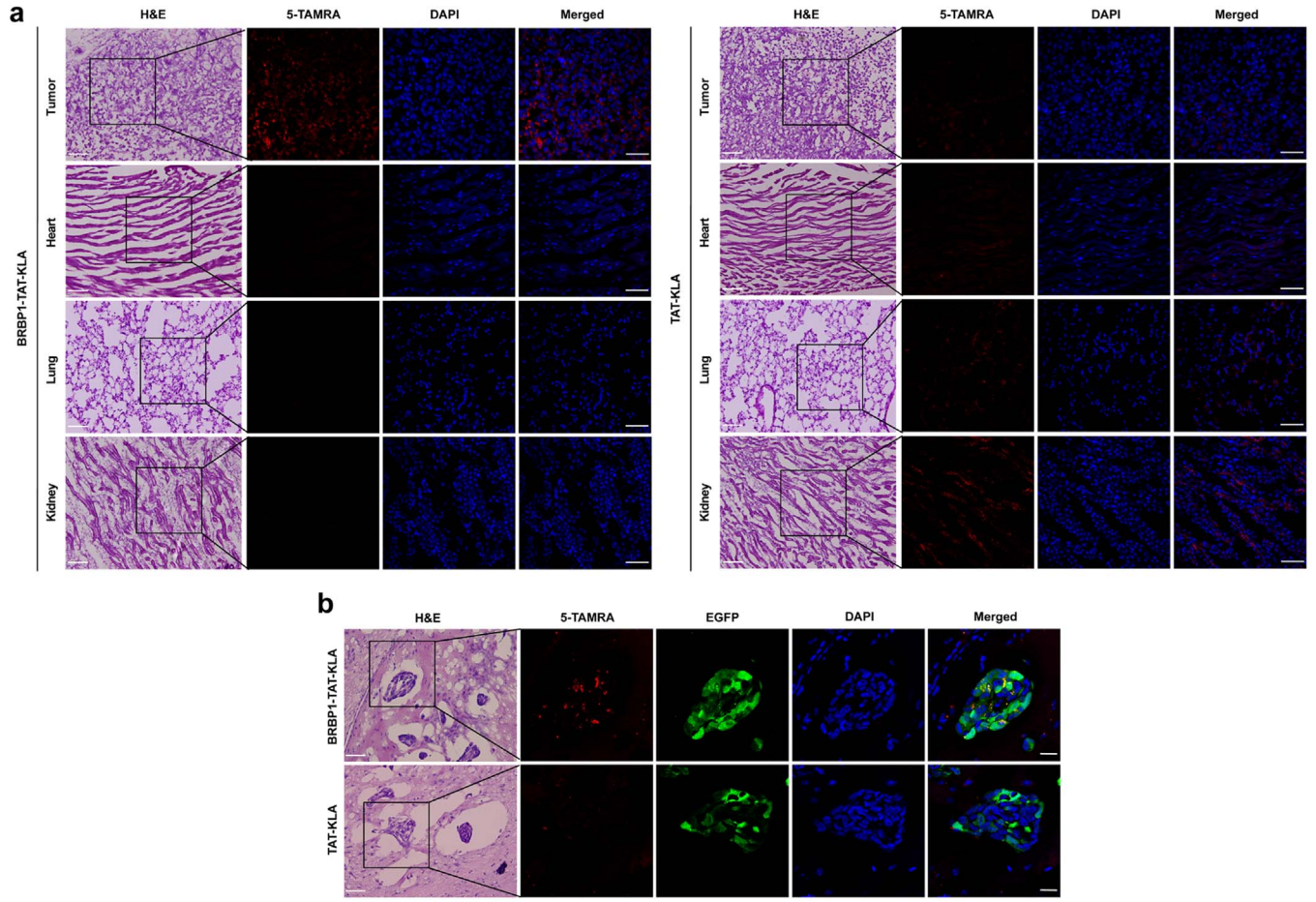

Figure 4 | ***In vivo* tumor homing of BRBP1-TAT-KLA.** 231-BR subcutaneous tumor model (a) and breast cancer brain metastasis model (b) were i.v injected with 1 nmol of BRBP1-TAT-KLA or TAT-KLA peptide labeled with 5-TAMRA and allowed to circulate for 1 h. Red color is from 5-TAMRA for the peptides, green color is from EGFP for the tumor cells, and blue color is from DAPI for nuclear visualization. Scale bars: (a) 50 μm; (b) 20 μm. (a) and (b) Each H&E staining overview (scale bars, 50 μm) is showed at the left panel and the fluorescence images corresponds to the black boxed area.

peptide to generate a biologically active agent. Compared with indirect-conjugated approaches (such as via drug carriermicelles, dendrimers, and liposomes), this direct-conjugated strategy has four advantages: (i) better escape from the vasculature; (ii) better diffusion through out the interstitial space of the tumor; (iii) ability to control peptide-drug ratio; (iv) lesser non-specific uptake in non-target cells[36]. However, this approach also has some limitations, such as lower drug load and rapid clearance rate[36].

Cell proliferation and apoptosis are common indicators for assessing the response of tumor cells to therapy[9]. Our findings demonstrated that exposure of 231-BR cells to BRBP1-TAT-KLA resulted in decreased cell viability and increased apoptosis, and that these effects were more dramatic than in the cells exposed to TAT-KLA alone. One possible explanation for this could be that BRBP1 exerted active targeting properties due to the specific binding of BRBP1-TAT-KLA to 231-BR cells. Subsequently, a higher concentration of the therapeutic agent was rapidly translocated across the cell membranes and internalized in the cells before they could be cleared or degraded. Our data also demonstrated that exposure of the human breast cancer cells MDA-MB-231 and BT-474 to BRBP1-TAT-KLA significantly inhibited cell viability compared with cells exposed to TAT-KLA alone, suggesting thereby that this molecularly targeted agent could also be effective for additional breast cancer subtypes. In addition to decreased cell viability, BRBP1-TAT-KLA also significantly inhibited the migration of 231-BR cells at subtoxic concentrations (1.25 μM and 2.5 μM). At these two concentrations, the peptide failed to exert significant toxic effects on cell viability (Figure 1b). Thus, we ruled out the possibility that decreased cell migration was not atributed to effects on cell viability. This finding is consistent with a previous report by Ma et al.[30] demonstrating that a KLA coupled peptide could inhibit the invasiveness of tumor cells *in vitro*. Our findings thus indicated that BRBP1-TAT-KLA exerted antitumor effects on human brain metastatic breast cancer cells through inhibition of cell viability as well as cell migraton *in vitro*.

KLA was originally designed as an antibacterial peptide[37] and it is relatively non-toxic in eukaryotic cells because it can not actively internalize in the cells[18,19]. It is well documented that once KLA is delivered into the cytoplasm of mammalian cells, it is able to induce mitochondrial disruption by triggering mitochondrial permeabilization and swelling, resulting in apoptosis[20,31,38]. Thus, efficient internalization of BRBP1-TAT-KLA is a prerequisite for exerting its cytotoxicity. Our results provided evidence that BRBP1-TAT-KLA efficiently internalized in the cytoplasm while not being distributed around the plasma membrane or in the nucleus. Following internalization, there were progressive changes in the mitochondrial morphology of 231-BR cells, from a state of enlarged matrix compartment and prominent cristae morphology to a state of swollen vesicle-like structures. Additionally, condensed cell nucleus and autophagosomes, all of which represent typical characteristics of cellular apoptosis[39], were also observed in BRBP1-TAT-KLA peptide-treated cells. It is well established that damaged mitochondria trigger apoptotic signaling cascades involving activation of caspases 9 and 3[20,31]. Consistent with these findings, we observed the cleavage of caspases 9 and 3 by western blotting in 231-BR cells treated with

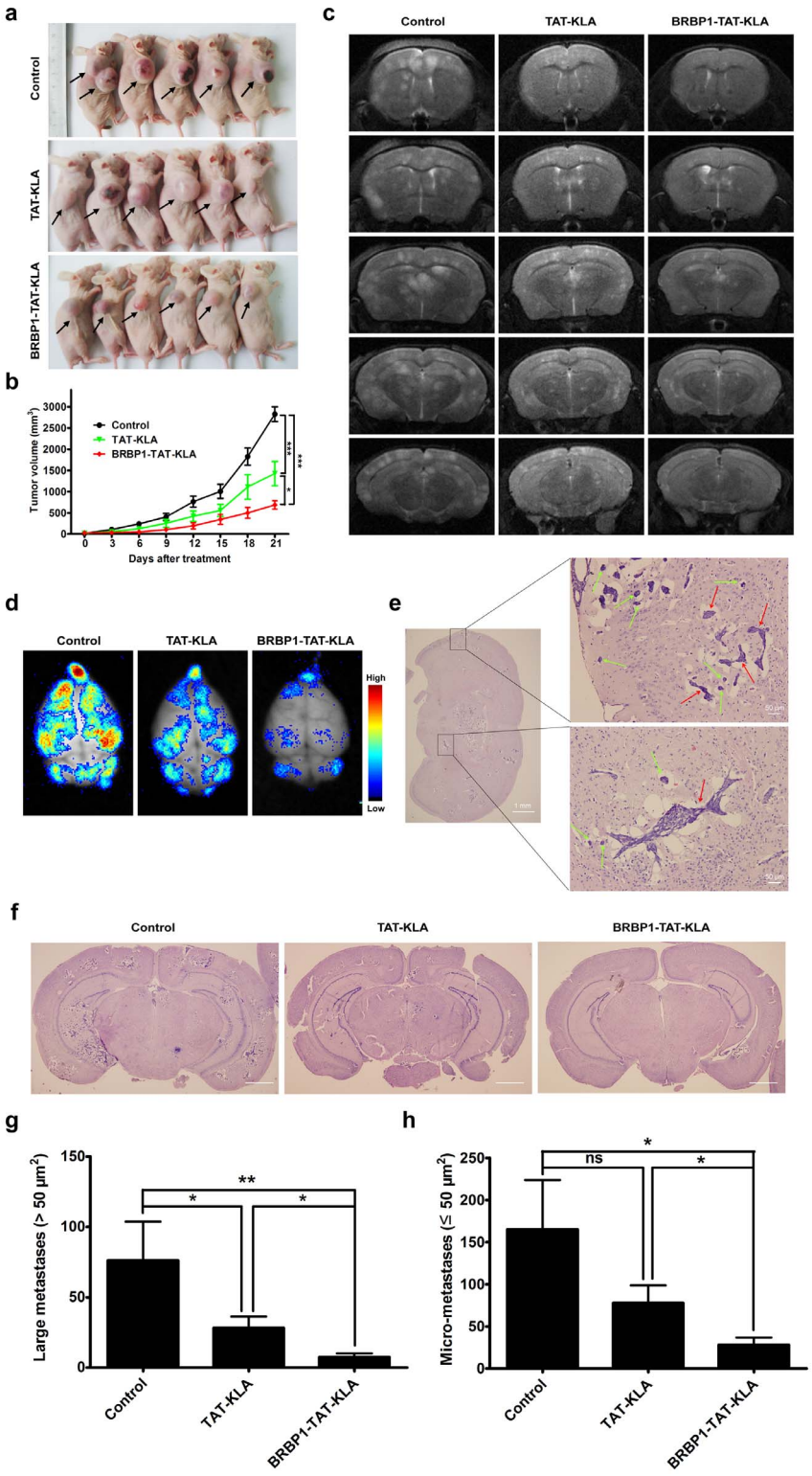

Figure 5 | BRBP1-TAT-KLA inhibited 231-BR tumor growth and outgrowth to the brain in mice. (a) and (b) Effect of BRBP1-TAT-KLA on tumor growth in the 231-BR subcutaneous tumor mice. The mice were i.v injected with BRBP1-TAT-KLA (n = 6), TAT-KLA (n = 6), or injection buffer (supplemented with DMSO in the same volume; n = 5) one time every three days. Tumor diameters were serially measured by calipers and tumor volumes (b) were dotted for analyzing the inhibition of BRBP1-TAT-KLA. (a) The images of the mice were taken on the twenty-first day after treatment. Black arrows indicate tumors. (c)-(h) Effect of BRBP1-TAT-KLA on the outgrowth of 231-BR cells to the brain in the breast cancer brain metastasis mice. Five days after tumor inoculation, the mice were administrated with BRBP1-TAT-KLA (n = 7), TAT-KLA (n = 7), or injection buffer (supplemented with DMSO in the same volume; n = 6) through tail vein injection every other day. Four weeks later, the brain metastases of the mice were assessed by MR imaging (c), *ex vivo* fluorescence imaging (d), and H&E staining (e)–(h). (e) H&E staining of the brain sections reveals brain lesions containing large metastases (red arrows) and micro-metastases (green arrows). (f) Representative H&E images of each group. Scale bars represent 1 mm. (g) and (h) Quantification of the number of large metastases (g) and micro-metastases (h). (b), (g) and (h) Data are represented as mean ± SEM. *, $P < 0.05$; **, $P < 0.01$; ***, $P < 0.001$; ns, not significant.

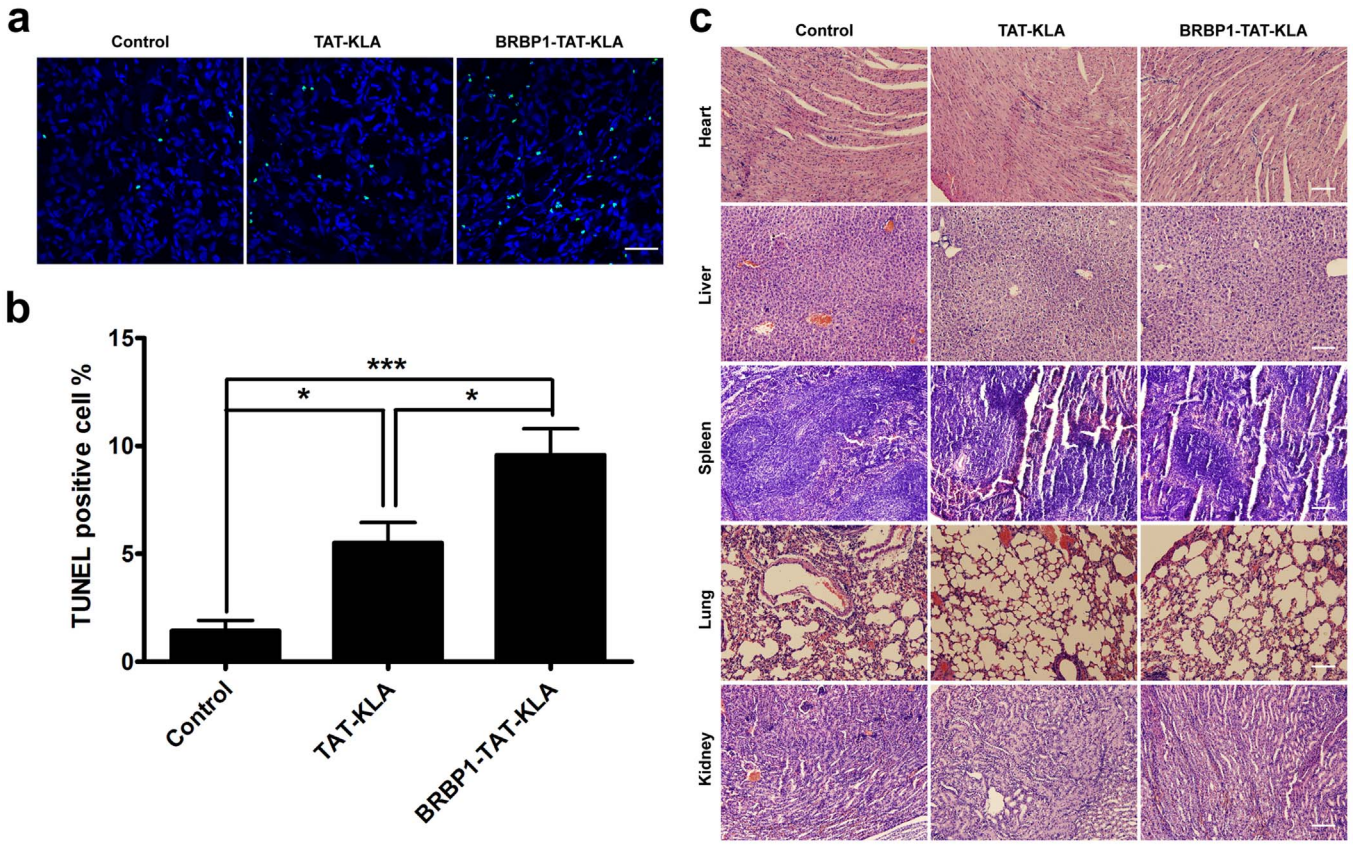

Figure 6 | Evaluation of tumor cellular apoptosis and potential side-effects of BRBP1-TAT-KLA in mice. (a) and (b) Tumor cellular apoptosis (green) detected by TUNEL staining assay following treatment in the 231-BR subcutaneous tumor mice. The cell nucleus were counterstained with DAPI (blue). (b) Quantification of the percentage of the TUNEL positive cells. Data are represented as mean ± SEM. n = 4. *, $P < 0.05$; ***, $P < 0.001$. (c) Histologic examination of vital tissues or organs (heart, liver, spleen, lung, and kidney) sections at the end of treatment in the breast cancer brain metastasis mice assessed by H&E staining. (a and c) Scale bars represent 50 μm.

BRBP1-TAT-KLA, suggesting thereby that mitochondria-mediated activation of caspases could, in part, be a pathway through which BRBP1-TAT-KLA exerted its effects on cell viability. These findings demonstrated that BRBP1-TAT-KLA efficiently internalized in 231-BR cells with subsequent induction of mitochondrial abnormal changes and initiation of cellular apoptosis involving activation of caspases 9 and 3.

Consistent with the findings *in vitro*, BRBP1-TAT-KLA significantly inhibited tumor growth and outgrowth to the brain *in vivo*. It must be mentioned that in the 231-BR subcutaneous tumor mice, while TAT-KLA was able to significantly decrease the tumor growth compared with the control group, inhibition of tumor growth was greater with the BRBP1-TAT-KLA peptide compared with the TAT-KLA peptide-treated group. Importantly, BRBP1-TAT-KLA failed to exert toxic effects on normal tissues (e.g., heart, liver, spleen, lung, and kidney) even at the end of the entire study. This specificity can be attributed to the fact that BRBP1-TAT-KLA preferentially bound to and accumulated in the 231-BR tumor compared with other normal organs (e.g., heart, lung, kidney) and that in the tumor tissue it induced cellular apoptosis compared with mice treated with either TAT-KLA or the control group. In addition to inhibiting tumor growth, BRBP1-TAT-KLA signifcantly inhibited the outgrowth of 231-BR cells to the brain as well. In the breast cancer brain metastasis mice, Gril et al.[27] reported that lapatinib was effective in inhibiting the development of large metastases. Consistent with this finding, we obsereved that TAT-KLA significantly inhibited the formation of large metastases. However, upon conjugating TAT-KLA with BRBP1, the resulting peptide not only significantly inhibited the formation of large metastases but also inhibited the foramtion of the micro-metastases in the breast cancer brain metastasis mice. This finding sheds light on the fact that that this agent could demonstrate clinical efficacy in adjuvant and/or preventive-based clinical settings. Enhanced inhibition of outgrowth of 231-BR cells to the brain for BRBP1-TAT-KLA may be due to the fact that the peptide more efficiently homed to the brain metastasis lesions compared with the homing of TAT-KLA as shown in the Figure 4b. Taken together, our data demonstrated that BRBP1-TAT-KLA is superior to TAT-KLA because it improves the specificity of the therapeutic agents for the cancer cells, thereby enhancing the antitumor effects while simultaneously reducing off-target side-effects.

Despite the encouraging results, some questions still remain unanswered, such as what are the receptor(s) or molecule(s) on the cell surface to which BRBP1-TAT-KLA binds, what are the mechanism(s) by which BRBP1-TAT-KLA inhibits cell migration *in vitro* and the outgrowth of the cells to the brain *in vivo*, and whether this compound peptide has inhibitory effect on preexisting brain metastases. Ongoing studies are underway to address these questions.

In summary, our findings indicated that BRBP1-TAT-KLA specifically targeted brain metastatic breast cancer, efficiently internalized in 231-BR cells, induced mitochondrial damage and cellular apoptosis. Furthermore, this peptide was able to significantly inhibit 231-BR tumor growth and outgrowth to the brain *in vivo*. BRBP1-TAT-KLA could thus be considered as a promising molecularly targeted therapeutic and (or) preventive strategy to augment current antitumor therapies.

Methods

Ethics statement. All experimental protocols were approved by the ethics committee of the Medical School of Southeast University, Nanjing, Jiangsu. The methods were carried out in accordance with the approved guidelines. All animal experiments were

conducted in accordance with the protocols evaluated and approved by Institutional Animal Care and Use Committee (IACUC) of the Medical School of Southeast University (approval ID: SYXK-2010.4987).

Cell lines and animal models. Human MDA-MB-231-BR "brain-seeking" breast carcinoma cell line (231-BR for brevity) was described previously[29]. The 231-BR cell line transfected with enhanced green fluorescent protein (EGFP) was kindly provided by Dr. Patricia S. Steeg (National Cancer Institute, National Institutes of Health, Bethesda, Md)[35]. The human breast cancer cells MDA-MB-231, BT-474, and MCF7, human normal mammary epithelial cells MCF 10A, human normal hepatic immortal cells HL-7702 were all purchased from the American Type Culture Collection (ATCC; Manassas, VA, USA). MCF 10A cells were cultured in Dulbecco's modified Eagle media/F12 (DMEM/F12; Invitrogen, San Diego, CA, USA) media supplemented with 10% horse serum, 20 ng/ml epidermal growth factor (EGF), 100 ng/ml cholera toxin, 0.01 mg/ml insulin, 500 ng/ml hydrocortisone and 1% penicillin-streptomycin solution. The other cells were cultured in DMEM (Invitrogen, San Diego, CA, USA) supplemented with 10% (v/v) fetal bovine serum (FBS; Invitrogen, San Diego, CA, USA). All the cells were cultured in a humidified incubator gassed with 5% CO_2 at 37°C.

Six-week-old female BALB/c nu/nu mice were obtained from Shanghai Slac Laboratory Animal Co, Ltd. (Shanghai, China). The breast cancer brain metastasis model was generated by injection of 231-BR(EGFP) cells (2×10^5 cells in 0.1 ml PBS) into the left cardiac ventricle of the mouse heart[34,35]. The subcutaneous tumor model was generated by subcutaneously injection (s.c) of 231-BR cells (5×10^6) into the right shoulder of the mouse.

Peptide design and synthesis. All peptides were synthesized and fluorescently labeled by GL Biochem (Shanghai., China) using standard solid-phase Fmoc chemistry. The products were purified to a minimum purity of 95% by high-performance liquid chromatography (HPLC) and isolated by lyophilization. The sequence and structure analysis of each peptide was characterized by mass spectrometry (MS). Totally five peptides including BRBP1 (MYPWTEPSYLSN), KLA ($D(KLAKLAK)_2$), BRBP1-KLA (MYPWTEPSYLSN-GG-$D(KLAKLAK)_2$), TAT-KLA (YGRKKRRQRRR-GG-$D(KLAKLAK)_2$), and BRBP1-TAT-KLA (MYPWTEPSYLSN-GG-YGRKKRRQRRR-GG-$D(KLAKLAK)_2$) were synthesized. The glycine residue groups served as spacers in each peptide, permitting loop formation[31,39]. The fluorescein 5-Carboxytetramethylrhodamine (5-TAMRA) was coupled to the peptides via an additional two glycine residues at the N-terminus. The peptides were all dissolved in dimethyl sulfoxide (DMSO; Sigma-Aldrich, St. Louis, MO, USA) and the vehicle control groups were supplemented with DMSO in the same volume.

MTT assay. Cells were respectively seeded in 96-well plates at a density of 5×10^3 cells/well. Twenty-four hours later, the cells were treated with BRBP1, KLA, BRBP1-KLA, TAT-KLA, BRBP1-TAT-KLA or DMSO (vehicle control) for 48 h. Then 50 μL of 3-(4, 5-dimethylthiazol-2-yl)-2, 5-diphenyltetrazolium bromide (MTT; 0.5 mg/mL) solution (Sigma-Aldrich, St. Louis, MO, USA) was added to each well. Four hours later, the medium was replaced by 200 μL of DMSO and the optical density (OD) was measured with a microplate reader (BIO-Rad, Hercules, California, USA) at wavelength of 570 nm. The percentage of cell viability was calculated using the following formula: % cell viability = (ODpositive)/(ODnegative), where ODpositive represents the OD570 value obtained from the peptide-treated group and ODnegative represents the OD570 value obtained from the corresponding vehicle control (the cells treated with DMSO in the equal volume).

Flow cytometry. 231-BR cells were treated with 10 μM of BRBP1, KLA, BRBP1-KLA, TAT-KLA, BRBP1-TAT-KLA, or DMSO (vehicle control) for 12 h. Apoptotic cells were stained using the Annexin V-FITC/Propidium Iodide (PI) Apoptosis Detection kit (Jiamay Biotech, Beijing, China) according to the manufacturer's procedure. Briefly, the cells were harvested and washed with 0.01 M phosphate-buffered saline (PBS) followed by centrifuge for 5 min at room temperature (RT). The cell pellets were resuspended in 1 × binding buffer and incubated with 5 μL Annexin V-FITC for 15 min. Subsequently, the cells were incubated with 5 μL PI for another 5 min. The apoptotic cells were assessed using a FACSCalibur flow cytometer (BD Bioscience, San Jose, CA, USA).

Immunofluorescent cell staining. 231-BR(EGFP) cells (5×10^4) were seeded onto coverslips coated with poly-L-lysine. Twenty-four hours later, the cells were washed twice with PBS and exposed to 5 μM BRBP1-TAT-KLA peptide labeled with 5-TAMRA for 30 min at 37°C. After washing 3 times, the cells were then fixed with 4% (w/v) paraformaldehyde (PFA) and counterstained with 4′, 6-diamidino-2-phenylindole (DAPI). The cells were washed another 2 times and mounted with glycerol-PBS (3 : 1). The slides were then observed under a laser scanning confocal microscope (Olympus Fluoview FV1000, Tokyo, Japan) to obtain the Z-stacks of the cells as described previously[40].

Transmission electron microscopy (TEM). 231-BR cells were cultured with BRBP1-TAT-KLA at varying concentrations (10, 20, and 30 μM) for 12 h. The cells were then harvested and fixed with a general fixative (containing 2% PFA and 2% glutaraldehyde in PBS, PH = 7.4) at 4°C overnight. After washing with PBS, the cells were dehydrated in a graded ethanol series of 50%, 70%, 85%, 95% and followed by rinse of 100% ethanol. Subsequently, the samples were infiltrated (first in propylene oxide/SPI-Pon 812 at 1 : 1 and 1 : 2, each for 1 h, and then in 100% SPI-Pon 812 for 1 h) and embedded in SPI-Pon 812 in three successive steps at 30°C, 42°C, and 60°C, each lasting for 24 h. The embedded samples were then sliced to a thickness of 80 nm. Finally, the ultrathin sections were stained with 2% uranyl acetate for 5 min and 2% lead citrate for 8 min. The samples were viewed and photographed with a Hitachi H-7650 TEM (Hitachi High-Technologies Corporation, Tokyo, Japan).

Western blotting. 231-BR cells were treated with either 10 μM or 20 μM BRBP1-TAT-KLA for 12 h, harvested, and lysed in a RIPA buffer (150 mM NaCl, 1% NP-40, 0.5% deoxycholate, 0.1% SDS, 50 mM Tris (pH 7.4), 10 mM sodium pyrophosphate, 100 mM sodium fluoride, 2 mM phenylmethylsulfonyl fluoride, and 1 mM DTT) with protease inhibitors (Roche, Mannheim, Germany). Subsequently, the total cell proteins were electrophoresed in a 10% sodium dodecyl sulfate-polyacrylamide gel (SDS-PAGE) followed by transfer to polyvinylidene difluoride (PVDF) membrane (Millipore, Bedford, MA, USA). After blocking with 3% (w/v) bovine serum albumin (BSA), the blots were probed with antibodies recognizing human caspase-3 (19 and 17 kDa), caspase-9 (37 kDa), and β-tubulin (55 kDa) (Cell Signaling Technology, MA, USA) overnight at 4°C. The secondary antibodies were horseradish peroxidase (HRP) conjugated goat anti mouse/rabbit IgG (Sigma-Aldrich, St. Louis, MO, USA). Signals were detected by chemiluminescence reagents (Pierce, Rockford, IL, USA) and imaged with a Tanon 5200 Imaging system (Shanghai, China). Quantification was performed by densitometry using Image J software (NIH).

***In vitro* migration assay.** The cell migration was examined using a transwell system (24-well insert; pore size, 8 μm; BD Biosciences) as previously reported[30], with some modifications. Briefly, 231-BR cells were treated with either 1.25 μM or 2.5 μM BRBP1-TAT-KLA peptide for 30 min, followed by plating the cells (5×10^4) in the upper chambers in serum-free medium. Lower chambers were filled with the medium supplemented with 10% (v/v) FBS. Twenty-four hours later, the cells that did not migrate through the pores were gently removed with cotton swabs. The cells on the lower surfaces of the membrane were fixed with cold methanol, stained with crystal violet (CV) staining solution and counted using an IX71 inverted microscope (Olympus, Tokyo, Japan).

***In vivo* tumor homing.** 231-BR subcutaneous tumor model and breast cancer brain metastasis model were intravenously (i.v) injected with 1 nmol of either BRBP1-TAT-KLA or TAT-KLA peptide labeled with 5-TAMRA, respectively. After 1 h of circulation, the mice were anesthetized with isoflurane (Shandong Keyuan Pharmaceuticals Company, Jinan, China). A catheter was introduced in the ascending aorta through a small cut on the left ventricle wall of the heart of the mouse, and perfusion was done with 30 ml PBS and then with 30 ml 4% (w/v) PFA through a cut in the auricula dextra. For the subcutaneous tumor mice, the tumors and organs (heart, lung, and kidney) were isolated. For the breast cancer brain metastasis mice, the brains were dissected. These tissues and organs were prepared for cryosectioning and serial sections of 10 μm-thickness were counterstained with DAPI, mounted, and photographed by a laser scanning confocal microscope (Olympus Fluoview FV1000, Tokyo, Japan).

Tumor growth and outgrowth to the brain. The 231-BR subcutaneous tumor mice were established as described above and used to investigate the effect of BRBP1-TAT-KLA on tumor growth. After the tumors reached ~50 mm^3 in volume, BRBP1-TAT-KLA (50 nmol in 100 μL PBS), TAT-KLA (50 nmol in 100 μL PBS) or injection buffer (DMSO in 100 μL PBS) was administered by tail vein injection every three days. Tumor growth was followed by caliper measurements of perpendicular measures of the tumor. Tumor volume was calculated using the formula: length × $width^2 \times 0.52$[41]. Once the mean value of tumor volume exceeded 2000 mm^3 in any of the groups, all the mice were sacrificed. The tumors were surgically removed for TUNEL assay and the organs (heart, liver, spleen, lung, and kidney) were excised for hematoxylin and eosin (H&E) staining.

The breast cancer brain metastasis mice were established as described above and used to investigate the effect of BRBP1-TAT-KLA on the outgrowth of 231-BR cells to the brain. Five days after the tumor cell transplantation, BRBP1-TAT-KLA (50 nmol in 100 μL PBS), TAT-KLA (50 nmol in 100 μL PBS) or injection buffer (DMSO in 100 μL PBS) was administered by tail vein injection every other day. Four weeks later, brain metastases in the mice were detected by magnetic resonance (MR) imaging. Afterwards, the mice were killed and the whole brain and organs (heart, liver, spleen, lung, and kidney) were surgically removed. The organs were subjected to H&E staining. The brains were subsequently to *ex vivo* fluorescence imaging and then to H&E staining. The H&E-stained brain serial sections that were cut every 1 mm through the whole brain were analyzed for the presence of metastatic lesions under light microscopy (Nikon, Tokyo, Japan). Every large metastasis (>50 μm^2) and micro-metastasis (≤50 μm^2) was counted in each section for quantification analysis as previously reported[27,34,35]. The >50 μm^2 for large metastases represents the mouse equivalent of the proportion of a MR imaging-detectable brain metastasis (5 mm) to the length of a human brain[27,35]. All analyses were carried out by 2 investigators who were blinded to experimental group assignment.

MR imaging. *In vivo* MR imaging was performed on a high magnetic field micro-MR research scanner (7.0T Bruker PharmaScans, Bruker Biospin, Ettlingen, Germany). Data acquisition and image processing were performed using a Paravision 5.0 software platform (Bruker Biospin, Ettlingen, Germany). The mice were anesthetized with 1.0% to 1.5% isoflurane with air and oxygen mixed at a 3 : 1 ratio. Respiratory

rate and body temperature were monitored using a physiology monitoring unit (Model 1025, SA Instruments Inc, Stony Brook, NY, US), and body temperature was maintained within physiologic limits using an animal warming system (MT1025, Bruker Biospin, Ettlingen, Germany). The T2-weighted images (T2-WI) were acquired using a turboRARE-T2 sequence and the imaging parameters were as follows: TR 2500 ms, TE 50 ms, FOV 2.0 × 2.0 cm, FA 180°, matrix size 256 × 256, and slice thickness of 1 mm (14 slices).

***Ex vivo* fluorescence imaging.** *Ex vivo* fluorescence images of whole brains were acquired using a Maestro *in vivo* imaging system (CRi, Woburn, MA, USA; Filter type, blue) and analysed using Maestro 2.10.0 Software (CRi, Woburn, MA, USA). All fluorescence images were acquired using 400 ms exposure time. The fluorescence signals were separated by multispectral imaging technology as reported previously[42].

H&E staining. The tissues or organs were dehydrated in graded alcohol, cleared through xylene for 10 min, and embedded in paraffin. The paraffin blocks were sectioned and stained with Harris modified hematoxylin (Fisher Scientific, Fair Lawn, NJ) followed by rinsing in running tap water, and then re-stained with eosin Y (Sigma-Aldrich, St. Louis, MO, USA), dehydrated, cleared, slide-mounted and visualized by a light microscope (Nikon, Tokyo, Japan).

TUNEL staining assay. For the TUNEL staining of cultured cells, 231-BR cells were treated with 20 μM of BRBP1, KLA, BRBP1-KLA, TAT-KLA, BRBP1-TAT-KLA, or DMSO in the same volume (control) for 24 h. The cells were fixed with 4% (w/v) PFA and permeabilized with 0.1% (v/v) Triton X-100. For the TUNEL staining of tissues, the tumors were fixed in 4% (w/v) PFA, cryo-protected in 30% (w/v) sucrose/PBS, embedded in OCT compound, and then serial sections of 10 μm-thickness were sectioned with a Leica CM 3050S cryostat. Tunnel staining was performed according to the manufacturer's instruction of the In Situ Cell Death Detection Kit, Fluorescein (Roche, Indianapolis, IN, USA). The nuclei of tumor cells were visualized by DAPI staining. The images were acquired by a laser scanning confocal microscope (Olympus Fluoview FV1000, Tokyo, Japan).

Statistical analysis. All in vitro experiments were repeated at least three times. The quantitative data were expressed as means ± standard error of the mean (SEM). The statistical analysis was performed using one-way ANOVA or Student's *t* test with the SPSS17 software package. $P < 0.05$ was defined as statistically significant.

1. Chien, A. J. & Rugo, H. S. Emerging treatment options for the management of brain metastases in patients with HER2-positive metastatic breast cancer. *Breast Cancer Res Treat* **137**, 1–12 (2013).
2. Larsen, P. B., Kumler, I. & Nielsen, D. L. A systematic review of trastuzumab and lapatinib in the treatment of women with brain metastases from HER2-positive breast cancer. *Cancer Treat Rev* **39**, 720–7 (2013).
3. Gil-Gil, M. J. *et al.* Breast cancer brain metastases: a review of the literature and a current multidisciplinary management guideline. *Clin Transl Oncol* **16**, 436–46 (2014).
4. Dawood, S. & Gonzalez-Angulo, A. M. Progress in the biological understanding and management of breast cancer-associated central nervous system metastases. *Oncologist* **18**, 675–84 (2013).
5. Lin, N. U. Targeted therapies in brain metastases. *Curr Treat Options Neurol* **16**, 276 (2014).
6. Patchell, R. A. & Regine, W. F. The rationale for adjuvant whole brain radiation therapy with radiosurgery in the treatment of single brain metastases. *Technol Cancer Res Treat* **2**, 111–5 (2003).
7. Nieder, C., Grosu, A. L. & Gaspar, L. E. Stereotactic radiosurgery (SRS) for brain metastases: a systematic review. *Radiat Oncol* **9**, 155 (2014).
8. Weber, G. F. Molecular mechanisms of metastasis. *Cancer Lett* **270**, 181–90 (2008).
9. Wang, T. *et al.* Enhanced tumor delivery and antitumor activity in vivo of liposomal doxorubicin modified with MCF-7-specific phage fusion protein. *Nanomedicine* **10**, 421–30 (2014).
10. Hatakeyama, S. *et al.* Targeted drug delivery to tumor vasculature by a carbohydrate mimetic peptide. *Proc Natl Acad Sci U S A* **108**, 19587–92 (2011).
11. Fu, B. *et al.* Identification and characterization of a novel phage display-derived peptide with affinity for human brain metastatic breast cancer. *Biotechnol Lett* **36**, 2291–301 (2014).
12. Fulda, S., Galluzzi, L. & Kroemer, G. Targeting mitochondria for cancer therapy. *Nat Rev Drug Discov* **9**, 447–64 (2010).
13. Wen, S., Zhu, D. & Huang, P. Targeting cancer cell mitochondria as a therapeutic approach. *Future Med Chem* **5**, 53–67 (2013).
14. Edeas, M. & Weissig, V. Targeting mitochondria: strategies, innovations and challenges: The future of medicine will come through mitochondria. *Mitochondrion* **13**, 389–90 (2013).
15. Lennon, F. E. & Salgia, R. Mitochondrial dynamics: biology and therapy in lung cancer. *Expert Opin Investig Drugs* **23**, 675–92 (2014).
16. Errico, A. Targeted therapy: Targeting mitochondria in pancreatic cancer. *Nat Rev Clin Oncol* **11**, 562 (2014).
17. Law, B., Quinti, L., Choi, Y., Weissleder, R. & Tung, C. H. A mitochondrial targeted fusion peptide exhibits remarkable cytotoxicity. *Mol Cancer Ther* **5**, 1944–9 (2006).
18. Agemy, L. *et al.* Targeted nanoparticle enhanced proapoptotic peptide as potential therapy for glioblastoma. *Proc Natl Acad Sci U S A* **108**, 17450–5 (2011).
19. Ellerby, H. M. *et al.* Anti-cancer activity of targeted pro-apoptotic peptides. *Nat Med* **5**, 1032–8 (1999).
20. Chen, W. H. *et al.* Dual-targeting pro-apoptotic peptide for programmed cancer cell death via specific mitochondria damage. *Sci Rep* **3**, 3468 (2013).
21. Cieslewicz, M. *et al.* Targeted delivery of proapoptotic peptides to tumor-associated macrophages improves survival. *Proc Natl Acad Sci U S A* **110**, 15919–24 (2013).
22. Farkhani, S. M. *et al.* Cell penetrating peptides: efficient vectors for delivery of nanoparticles, nanocarriers, therapeutic and diagnostic molecules. *Peptides* **57**, 78–94 (2014).
23. Rayapureddi, J. P., Tomamichel, W. J., Walton, S. T. & Payne, R. M. TAT fusion protein transduction into isolated mitochondria is accelerated by sodium channel inhibitors. *Biochemistry* **49**, 9470–9 (2010).
24. Kim, H. Y. *et al.* The cell penetrating ability of the proapoptotic peptide, KLAKLAKKLAKLAK fused to the N-terminal protein transduction domain of translationally controlled tumor protein, MIIYRDLISH. *Biomaterials* **32**, 5262–8 (2011).
25. Kwon, M. K. *et al.* Antitumor effect of a transducible fusogenic peptide releasing multiple proapoptotic peptides by caspase-3. *Mol Cancer Ther* **7**, 1514–22 (2008).
26. Yang, H. *et al.* Chondroitin sulfate as a molecular portal that preferentially mediates the apoptotic killing of tumor cells by penetratin-directed mitochondria-disrupting peptides. *J Biol Chem* **285**, 25666–76 (2010).
27. Gril, B. *et al.* Effect of lapatinib on the outgrowth of metastatic breast cancer cells to the brain. *J Natl Cancer Inst* **100**, 1092–103 (2008).
28. Zhao, H. *et al.* The effect of mTOR inhibition alone or combined with MEK inhibitors on brain metastasis: an in vivo analysis in triple-negative breast cancer models. *Breast Cancer Res Treat* **131**, 425–36 (2012).
29. Yoneda, T., Williams, P. J., Hiraga, T., Niewolna, M. & Nishimura, R. A bone-seeking clone exhibits different biological properties from the MDA-MB-231 parental human breast cancer cells and a brain-seeking clone in vivo and in vitro. *J Bone Miner Res* **16**, 1486–95 (2001).
30. Ma, X. *et al.* Anti-tumor effects of the peptide TMTP1-GG-D(KLAKLAK)(2) on highly metastatic cancers. *PLoS One* **7**, e42685 (2012).
31. Li, K. *et al.* Targeting acute myeloid leukemia with a proapoptotic peptide conjugated to a Toll-like receptor 2-mediated cell-penetrating peptide. *Int J Cancer* **134**, 692–702 (2014).
32. Askoxylakis, V. *et al.* Preclinical evaluation of the breast cancer cell-binding peptide, p160. *Clin Cancer Res* **11**, 6705–12 (2005).
33. Askoxylakis, V. *et al.* Characterization and development of a peptide (p160) with affinity for neuroblastoma cells. *J Nucl Med* **47**, 981–8 (2006).
34. Nie, F. *et al.* Involvement of epidermal growth factor receptor overexpression in the promotion of breast cancer brain metastasis. *Cancer* **118**, 5198–209 (2012).
35. Palmieri, D. *et al.* Her-2 overexpression increases the metastatic outgrowth of breast cancer cells in the brain. *Cancer Res* **67**, 4190–8 (2007).
36. Brown, K. C. Peptidic tumor targeting agents: the road from phage display peptide selections to clinical applications. *Curr Pharm Des* **16**, 1040–54 (2010).
37. Javadpour, M. M. *et al.* De novo antimicrobial peptides with low mammalian cell toxicity. *J Med Chem* **39**, 3107–13 (1996).
38. Alves, I. D. *et al.* A proapoptotic peptide conjugated to penetratin selectively inhibits tumor cell growth. *Biochim Biophys Acta* **1838**, 2087–98 (2014).
39. Liu, R. *et al.* Enhanced targeted anticancer effects and inhibition of tumor metastasis by the TMTP1 compound peptide TMTP1-TAT-NBD. *J Control Release* **161**, 893–902 (2012).
40. Wang, T. *et al.* Targeted cell uptake of a noninternalizing antibody through conjugation to iron oxide nanoparticles in primary central nervous system lymphoma. *World Neurosurg* **80**, 134–41 (2013).
41. He, X. *et al.* A novel peptide probe for imaging and targeted delivery of liposomal doxorubicin to lung tumor. *Mol Pharm* **8**, 430–8 (2011).
42. Zhang, Y. *et al.* In vivo near-infrared imaging of fibrin deposition in thromboembolic stroke in mice. *PLoS One* **7**, e30262 (2012).

Acknowledgments

This research was supported by National Basic Research Program of China (973 program; 2013CB733801), National Nature Science Foundation of China (81371609) and Research and innovation program of Jiangsu Province, China (CXLX12_0073). The authors gratefully acknowledge Prof. Honghong Yao (Medical School of Southeast University), Dr. Shilpa Buch (University of Nebraska Medical Center), and Dr. Michael T. Maloney (Stanford University School of Medicine) for editing the manuscript.

Author contributions

J.Z. and G.T. designed the research, B.F., W.L., Y.Z., A.Z., F.M. and G.G. performed the experiments, Y.S., N.P., F.N. and Y.H. analyzed the data, and B.F. wrote the main manuscript text and prepared all of the figures. All of the authors reviewed and approved the manuscript.

Additional information

Supplementary information accompanies this paper at http://www.nature.com/scientificreports

Competing financial interests: The authors declare no competing financial interests.

How to cite this article: Fu, B. *et al.* Enhanced antitumor effects of the BRBP1 compound peptide BRBP1-TAT-KLA on human brain metastatic breast cancer. *Sci. Rep.* **5**, 8029; DOI:10.1038/srep08029 (2015).